Nanoscale mapping and functional analysis of individual adhesins on living bacteria

Vincent Dupres[1,7], Franco D Menozzi[2,3,7], Camille Locht[3], Brian H Clare[4], Nicholas L Abbott[4], Stéphane Cuenot[5], Coralie Bompard[6], Dominique Raze[2,3] & Yves F Dufrêne[1]

Although much progress has been made in the identification and characterization of adhesins borne by pathogenic bacteria, the molecular details underlying their interaction with host receptors remain largely unknown owing to the lack of appropriate probing techniques. Here we report a method, based on atomic force microscopy (AFM) with tips bearing biologically active molecules, for measuring the specific binding forces of individual adhesins and for mapping their distribution on the surface of living bacteria. First, we determined the adhesion forces between the heparin-binding haemagglutinin adhesin (HBHA) produced by *Mycobacterium tuberculosis* and heparin, used as a model sulphated glycoconjugate receptor. Both the adhesion frequency and adhesion force increased with contact time, indicating that the HBHA-heparin complex is formed via multiple intermolecular bridges. We then mapped the distribution of single HBHA molecules on the surface of living mycobacteria and found that the adhesin is not randomly distributed over the mycobacterial surface, but concentrated into nanodomains.

M. tuberculosis, the worldwide leading causative agent of death owing to a single etiologic agent, adheres to epithelial cells via the HBHA, a 199-residue protein that recognizes heparan sulphate proteoglycans (HSPG). Besides the *M. tuberculosis* complex members[1,2], other pathogenic mycobacteria, such as *Mycobacterium leprae* (F.D.M. and M.C. Vidal-Pessolani, unpublished data; http://genolist.pasteur/leproma) and *Mycobacterium avium* also produce HBHA-related molecules[3]. Non-pathogenic mycobacteria, such as *Mycobacterium smegmatis* produce only distantly-related HBHA-like proteins (F.D.M. and F. Biet, unpublished data; http://www.tigr.org/tigr-scripts/CMR2/CMRGenomes.spl). *M. tuberculosis* HBHA has been shown to be involved (i) in the mycobacterial interaction with epithelial cells, but not with professional phagocytes[4,5], and (ii) in the extrapulmonary dissemination of the bacilli by a mechanism that still remains to be explained[5,6]. The HBHA-mediated adherence relies on the interaction of its C-terminal lysine-rich domain with HSPG receptors present on the surface of its target cells[2,7]. Grafting of the C-terminal lysine-rich domain onto heterologous proteins has revealed that the entire adherence determinant of HBHA is located in this roughly 50-residue region, consisting of two identical repeats exclusively composed of alanines, lysines and prolines[2]. The affinity of this lysine-rich repeat region to model sulphated glycoconjugates, such as heparin, has been determined by surface plasmon resonance to be in the nanomolar range[2].

In the past decade, AFM[8] has emerged as a powerful tool to image biological structures at high resolution[9–11] and to measure the forces within or between single biomolecules[11–15]. In particular, functionalization of the AFM tip with ligands has allowed mapping the distribution of complementary receptors on model or cellular surfaces[16–20]. Here we used AFM to measure the specific interaction forces between HBHA and its receptor at the single-molecule level. We demonstrated that the HBHA-heparin adhesion forces have a bimodal distribution and increase with contact time, suggesting the interaction involves multiple intermolecular bridges. We also demonstrated that the approach can be used to map single HBHA molecules on the surface of living mycobacteria, revealing that the adhesin is localized in discrete regions of the cell surface. Virtually applicable to any microbial adhesin, the nanoscale functional imaging of living cells presented here provides new opportunities for explaining cellular interaction processes at the single-molecule level.

RESULTS

Attaching HBHA and heparin to AFM tips and substrates

To probe the HBHA-heparin interaction force, recombinant HBHA bearing a His tag at its N-terminal end (rHBHA N-His)[7] was attached to gold-coated AFM tips bearing Ni^{2+}-nitrilotriacetate (NTA) groups[21], and biotinylated heparin molecules were immobilized onto plane gold substrates via a sandwich layer of streptavidin and biotinylated bovine serum albumin (BBSA; **Fig. 1a**). To validate the quality of the functionalized surfaces, gold substrates
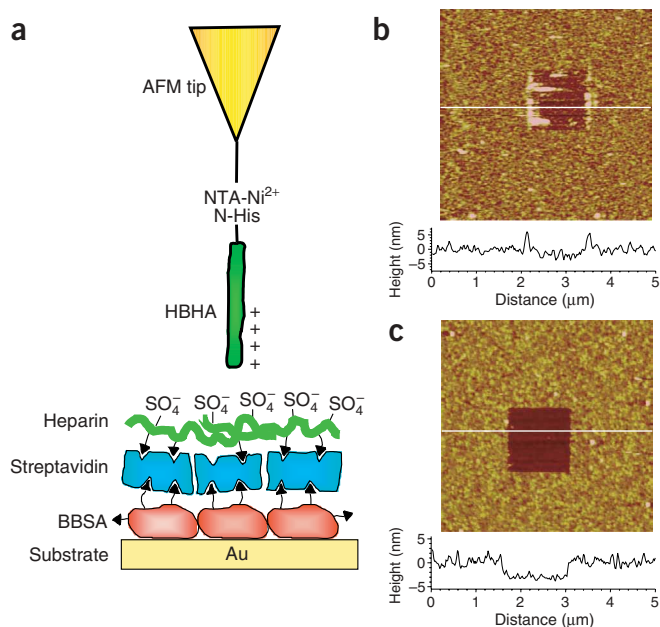
Figure 1 | Strategy for measuring the HBHA-heparin binding force at the single-molecule level using AFM. (**a**) Schematics of the surface chemistry used to functionalize the AFM tip and substrate with HBHA and heparin. Recombinant histidine-tagged HBHA (rHBHA N-His) were attached to an AFM tip terminated with Ni^{2+}-NTA and EG3 groups, and biotinylated heparin was bound to a gold substrate via streptavidin and BBSA layers. (**b,c**) AFM images of the biologically-modified substrates in PBS confirming the presence of smooth, homogeneous HBHA (**b**) and heparin (**c**) layers. Data from cross-sections taken along the white lines are displayed under the images. To determine the layer thicknesses, 1 μm × 1 μm square areas were first scanned at large forces (10 nN), and then 5 μm × 5 μm squares of the same areas were imaged under smaller forces.

coated with HBHA or heparin were imaged by AFM in phosphate-buffered saline (PBS; **Fig. 1b,c**). The morphology of both surfaces was homogeneous, smooth and stable upon repeated scanning, indicating strong attachment of HBHA and heparin to the gold surfaces. This was confirmed by scanning small areas (1 μm × 1 μm) at large forces (10 nN), which resulted in the removal of the biomolecular layers and allowed us to directly determine their thickness (1 ± 0.1 nm and 4 ± 1 nm for HBHA and heparin-streptavidin layers, respectively).

Measuring the interaction forces of the HBHA-heparin pair
We recorded force-distance curves at a loading rate of 10,000 pN/s between the HBHA tip and the heparin-coated surface (**Fig. 2a**). Adhesion forces were detected in 32% of a total of 1,000 curves. The

adhesion force histogram revealed a bimodal distribution with average rupture forces of 50 ± 23 pN and 117 ± 18 pN. The rupture length of the adhesion events ranged from 10 to 55 nm, which is consistent with the elasticity of polysaccharide chains like heparin[22]. To determine the specificity of the measured interaction, (i) force-distance curves between the HBHA tip and the heparin-coated surface were recorded in a 50 μg/ml heparin solution, and (ii) the HBHA tip was replaced by a bovine serum albumin (BSA)-coated tip. Both the presence of free heparin and the use of a BSA tip dramatically reduced the number of curves showing adhesion events, as well as the measured binding forces (**Fig. 2b,c**), indicating that the adhesion forces measured using the HBHA tip are specific to the HBHA-heparin interaction.

Exploring the dynamics of the HBHA-heparin interaction
To investigate the dynamics of the HBHA-heparin interaction, force curves between the HBHA tip and the heparin-coated surface were recorded at various retraction rates and contact times (**Fig. 3**). The mean adhesion force did not substantially depend on the loading rate applied during retraction, over the experimentally accessible range (**Fig. 3a**). This observation, in contrast to the behavior of several other receptor-ligand complexes that usually have an increase in the adhesion force with the logarithm of the loading rate[23,24], indicates that the force measurements were done
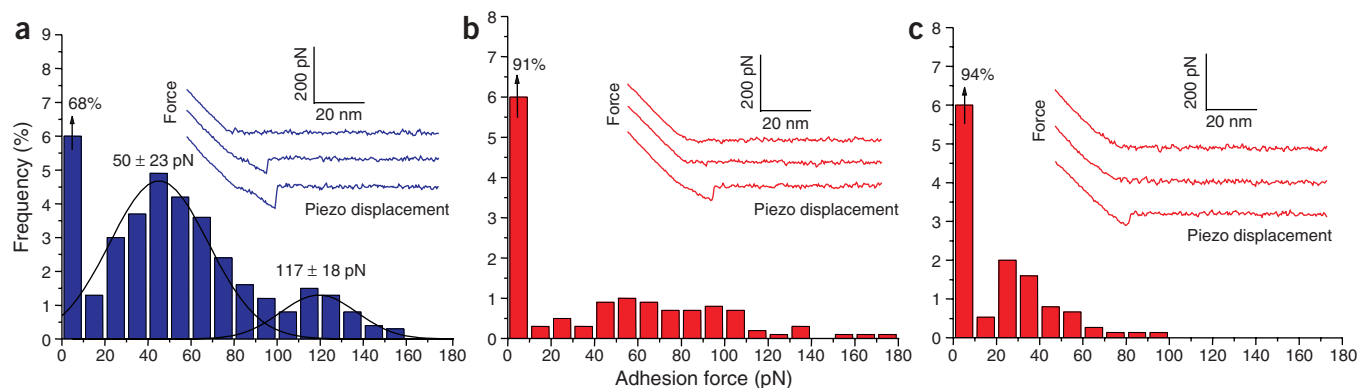

Figure 2 | Measurement of the binding force of the HBHA-heparin complex. (**a**) Force curves and adhesion force histogram obtained in PBS between a HBHA tip and a heparin substrate. The curves are three representative examples from a total of 1,000 force curves obtained using independent tips and substrates. The adhesion force histogram obtained from the 1,000 force curves ($n = 1,000$) reveals a bimodal distribution of adhesion forces with maxima at 50 ± 23 pN and 117 ± 18 pN, as determined by a Gaussian fit. As indicated by the arrow, 68% of the curves show no adhesion. (**b**) Force curves and adhesion force histogram ($n = 1,000$) obtained after injection of free heparin (50 μg/ml) in the solution. The dramatic reduction of adhesion frequency and broadening of the distribution reflect the blocking of the HBHA adhesion sites. (**c**) Force curves and histogram ($n = 1,000$) obtained using a BSA tip. The reduction of adhesion probability and adhesion force is attributed to the nonspecific adhesion between the BSA and heparin surfaces. All the curves were obtained using a loading rate of 10,000 pN/s (both during approach and retraction) and an interaction time of 500 ms. Similar data were obtained using more than ten different probes and independent samples.
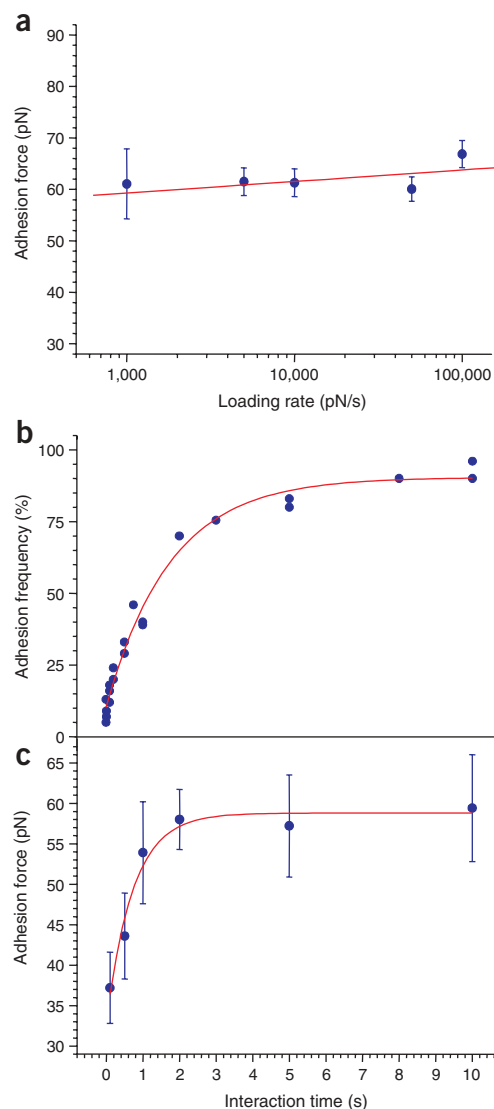
Figure 3 | Dynamics of the HBHA-heparin interaction. (**a**) Dependence of the adhesion force on the loading rate applied during retraction, measured between a HBHA tip and a heparin substrate, while keeping constant the interaction time (500 ms) and the loading rate during approach (10,000 pN/s). The mean adhesion force does not notably change with the loading rate. (**b,c**) Dependence of the adhesion frequency (**b**) and adhesion force (**c**) on the interaction time, measured at a constant loading rate of 10,000 pN/s during approach and retraction. Both adhesion probability and adhesion force increase exponentially with interaction time. Data in **a,c** represent the mean ± s.e.m. (**a**, $n = 100$; **c**, $n = 200$).

scanning electron microscopy observations[26]. Using a heparin tip, 1,024 force-distance curves were recorded across the cell surface, and the curves showed adhesion forces in about half of the cases (**Fig. 4c**). These forces again had a bimodal distribution with mean values of 53 ± 18 pN and 110 ± 11 pN that matched remarkably well with the data obtained using purified HBHA immobilized on gold surface (**Fig. 2a**). Two sets of experiments confirmed the specificity of the measured interaction. First, 1,024 force curves recorded in the presence of free heparin showed a marked reduction of adhesion frequency (from 49% to 4%; data not shown). Second, although a mutant *M. bovis* BCG strain lacking HBHA, had a smooth and homogeneous surface comparable to that of the parental strain (data not shown), it did not bind the heparin tip substantially (**Fig. 4e**). Taken together, these observations suggest that the measured binding forces are specific of the HBHA-heparin interaction, the heparin-binding region of HBHA is surface-exposed and the HBHA-heparin interaction most likely occurs through multiple intermolecular bridges.

To address the HBHA distribution on the *M. bovis* BCG surface, spatially-resolved adhesion maps were recorded using a heparin tip over 300 nm × 300 nm areas with a lateral resolution of 20 nm (**Figs. 4d** and **5a**). In about half of the locations, the mapping revealed adhesion events (clear pixels) owing to the presence of HBHA molecules, as these events were not observed in experiments with the mutant deficient in HBHA production (**Figs. 4f** and **5b**). Notably, the HBHA distribution was not homogeneous, but apparently concentrated into nanodomains that may have important biological functions.

DISCUSSION

The results presented here demonstrate that AFM with tips bearing biologically active molecules is a powerful tool for measuring the adhesion forces that trigger cognate interactions in microbiological processes, and for mapping, at the nanometer level, functional molecules present on the surface of living bacteria. The strategy for measuring the specific HBHA-heparin interaction forces at the single-molecule level involved attaching recombinant histidine-tagged HBHA onto an AFM tip terminated with Ni^{2+}-NTA and EG3 groups and binding biotinylated heparin to a gold substrate via streptavidin and BBSA layers (**Fig. 1**). The HBHA coupling approach offers several advantages, as it allows an optimal exposure of the C-terminal adhesive domain, confers high mobility to the attached adhesin, minimizes nonspecific protein adsorption and allows low-density coupling to ensure single-molecule recognition[13,21].

The bimodal distribution of the specific adhesion forces (**Fig. 2a**) reflects the occurrence of one and two binding events between HBHA and heparin, as has been reported for other receptor-ligand

close to thermodynamic equilibrium[25]. We then varied the contact time (few ms to 10 s), while keeping the loading rate during approach and retraction constant (10,000 pN/s). Under these conditions, the adhesion frequency (that is, the number of curves with adhesion events) increased exponentially with contact time and reached a plateau after 5 s (**Fig. 3b**). This type of interaction is reminiscent of that described for the vascular endothelial cadherin[24] involved in intercellular adhesion within endothelial barriers, except that for this protein the plateau was reached after 0.2 s, indicating that bond formation is much faster. We also observed that the HBHA-heparin adhesion force increased exponentially with contact time (**Fig. 3c**). Accordingly, the dependence of adhesion frequency and adhesion force on contact time suggests that the HBHA-heparin complex is formed via multiple intermolecular electrostatic bridges.

Mapping single adhesins on living mycobacteria

We used AFM to explore the surface of living *Mycobacterium bovis* bacillus Calmette Guérin (BCG) immobilized on a polycarbonate membrane (**Figs. 4** and **5**). Topographic images revealed a smooth and homogeneous surface (**Fig. 4a,b**), which is consistent with
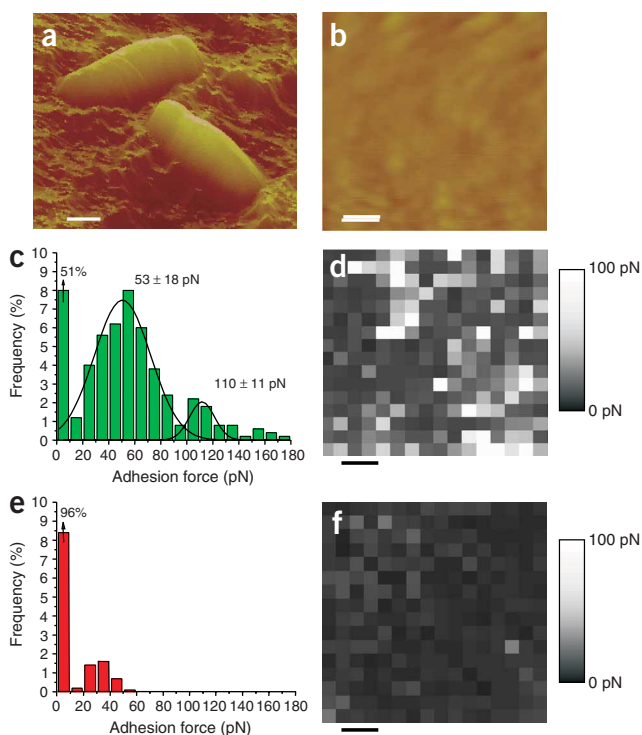
Figure 4 | Mapping single HBHA adhesins on living mycobacteria. (**a**) AFM topographic image recorded in PBS showing two *M. bovis* BCG cells on a polymer substrate. Scale bar, 1 μm. (**b**) High-resolution image of the cell surface revealing a smooth, homogeneous morphology. Scale bar, 50 nm. (**c,d**) Histogram (obtained from 1,024 force curves; $n = 1,024$) and spatially-resolved map of adhesion forces recorded with a heparin tip with a constant pulling rate (10,000 pN/s both during approach and retraction) and interaction time (500 ms). Scale bar, 50 nm. The 53 pN adhesion forces reflect the detection of single HBHA monomers while the 110 pN forces may correspond to single dimers or two monomers. (**e,f**) Control experiment: adhesion force histogram ($n = 1,024$) and map obtained for a *M. bovis* BCG mutant strain deficient for HBHA production (*M. bovis* BCG Δ*HBHA*). Scale bar, 50 nm.

natural infection, *M. tuberculosis* may exhibit broad-range epithelial adherence behaviors that could represent an adaptive trait by favoring bacterial aggregation or dissemination.

Using heparin tips, we detected single HBHA molecules on the surface of living *M. bovis* BCG cells (**Figs. 4c,d** and **5a**). Notably, spatially-resolved adhesion maps revealed that the HBHA-mediated heparin binding activity is not randomly distributed over the mycobacterial surface, but apparently concentrated into nanodomains for which we propose the term adherosome. As HSPG-binding adhesins may induce oligomerization of their receptors upon binding[29] and the recruitment of these receptors within membrane rafts[30], the clustering of HBHA at the mycobacterial surface may promote adhesion to target cells. Such an hypothesis will clearly deserve further investigation. There are other exciting issues to address in future AFM research, which include assessing whether the partitioning is a specific property of HBHA or reflects the organization of other bacterial surface proteins, and whether the HBHA concentration at the cell pole differs from that on the rest of the bacterial surface.

In conclusion, the present study demonstrates that AFM is a valuable method for exploring the interaction forces of bacterial adhesins and for assessing their distribution on the surface of living cells. This nanoscale approach offers two major advantages over existing high-resolution imaging techniques. First, the

pairs, for which a proportional increase of the interaction forces has been shown to be due to the presence of multiple binding sites[27]. The ∼50 pN binding force may correspond to the interaction strength quantum between heparin and a monomeric form of HBHA, whereas the ∼117 pN force may be due either to the simultaneous interaction of two single HBHA molecules or to the binding of an HBHA dimer. Indeed, based on its amino acid sequence, the N-terminal domain of HBHA has been predicted to contain a coiled-coil region, which could potentially be involved in homotypic interactions leading to dimerization[7]. Moreover, gel filtration analysis of purified HBHA indicates that the adhesin can form dimers (F.D.M., unpublished data).

Our finding that the adhesion frequency and adhesion force increase with contact time (**Fig. 3b,c**) is consistent with the formation of multiple intermolecular bridges between HBHA and its receptor. As a matter of fact, the prolonged contact time required to establish strong HBHA-heparin interaction would reflect the time necessary for conformational changes within both molecules to allow an optimal fitting between the positive charges of the HBHA heparin-binding domain and the sulphate groups of heparin[28]. This model is consistent with the fact that the HBHA affinity for heparin directly correlates with the number of the lysine-rich repeats in the heparin-binding site of HBHA[2]. As the number of electrostatic bridges between HBHA and heparin modulates the strength of the complex, it suggests that, during

Figure 5 | Distribution of HBHA on the surface of *M. bovis* BCG and *M. bovis* BCG Δ*HBHA* as probed using different tips and cell preparations. (**a,b**) Adhesion force maps (gray scale as in **Fig. 4d,f**) recorded with heparin tips over *M. bovis* BCG cells (**a**) and mutant *M. bovis* BCG cells deficient in HBHA production (**b**). Data obtained using eight different tips on 16 mycobacteria from six independent samples. Scale bars, 100 nm.
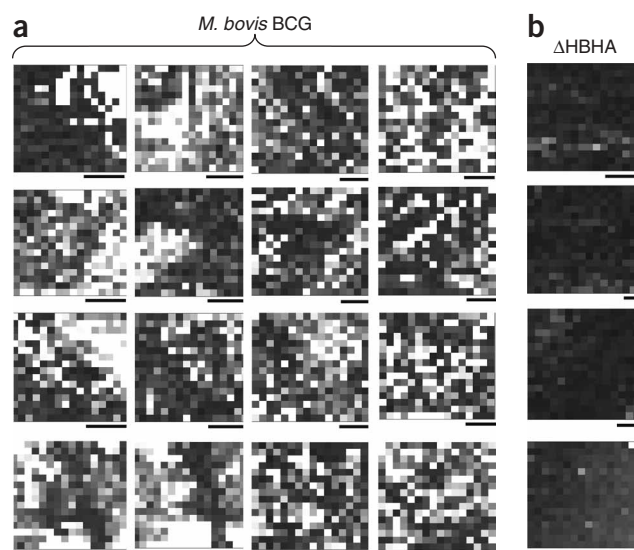
investigations are noninvasive and performed directly in aqueous solution without any cell pretreatment, thus preserving the native organization and conformation of the surface molecules; second, it allows a functional analysis of single cell-surface molecules. In future research, the use of biologically modified tips should shed new light on the molecular bases of microbial adhesion processes, and may help in the development of new drugs capable of blocking the adhesin-receptor interaction[31]. Promising applications are also expected in other fields, such as environmental microbiolgy in which, for instance, the technique should contribute to the understanding of biofilm formation.

METHODS

Bacterial cultures and protein purification. *M. bovis* BCG and its isogenic mutant strain deficient in HBHA production[5] were grown in Sauton medium as described[1]. *Escherichia coli* BL21(pGD51) producing rHBHA N-His has been described elsewhere[7], and the recombinant protein was purified by heparin Sepharose chromatography[1].

Preparation of HBHA tips and substrates. To attach purified rHBHA N-His onto Ni^{2+}-NTA–terminated AFM tips and silicon substrates, AFM cantilevers and silicon wafers (Siltronix) were coated using electron beam thermal evaporation with a 5-nm thick chromiumé layer followed by a 30-nm thick gold layer. The gold-coated surfaces were cleaned for 5 min by UV and ozone treatment (Jelight Co.), rinsed with ethanol, dried with a gentle nitrogen flow and immersed overnight in ethanol containing 0.05 mM of NTA-terminated (20%) and tri(ethylene glycol(EG))-terminated (80%) alkanethiols[21]. After rinsing with ethanol, the samples coated with alkanethiols were immersed in a 40 mM aqueous solution of $NiSO_4$ (pH 7.2) for 1 h, rinsed with PBS, incubated in a PBS solution containing 2 µM rHBHA N-His for 2 h, and finally rinsed with PBS. The functionalized surfaces were always kept hydrated and used immediately after preparation.

Preparation of heparin tips and substrates. Gold-coated cantilevers and substrates were immersed overnight at room temperature in a 25 µg/ml solution of BBSA (Sigma) in PBS. After rinsing with PBS, the BBSA surfaces were exposed to a 10 µg/ml solution of streptavidin (Sigma) in PBS for 2 h followed by thorough rinsing with PBS. Finally, the BBSA-streptavidin surfaces were immersed for 2 h in a PBS solution containing 10 µg/ml biotinylated heparin (Sigma) and rinsed with PBS.

AFM measurements. To probe mycobacteria in their native state by AFM, the bacteria were mechanically immobilized onto Isopore polycarbonate membranes (Millipore), an approach that permits the imaging of single cells under aqueous conditions while minimizing denaturation of the specimen[11]. After filtering a concentrated cell suspension, the membrane was first imaged at low resolution (typically 20 µm × 20 µm) to identify single bacteria. Then, by reducing the image size progressively, high-resolution topographic images and adhesion force maps (300 nm × 300 nm size) could be recorded at the surface of individual cells. A topographic image was always recorded after a force mapping to confirm that the force measurements were nondestructive.

AFM contact mode images and force-distance curves were obtained using a Nanoscope IV Multimode AFM (Veeco Metrology Group). Measurements were performed in PBS solutions at room temperature using triangular silicon nitride cantilevers (Microlevers, Veeco Metrology Group). Unless otherwise specified, all force measurements were recorded with a loading rate of 10,000 pN/s, calculated by multiplying the tip pulling velocity (nm/s) by the spring constant of the cantilever (pN/nm). Blocking experiments were performed with a heparin solution (50 µg/ml in PBS). BSA tips were prepared by incubating gold-coated cantilevers overnight in a BSA solution (25 µg/ml in PBS) and then rinsing with PBS.

The spring constants of the cantilevers were estimated as follows. The geometrical dimensions of each functionalized cantilever were accurately measured by scanning electron microscopy, and their free resonance frequency was measured. Then, their mechanical properties were adjusted to match the calculated frequencies to the measured ones. The determined mechanical properties and the measured geometrical dimensions were then used to calculate the spring constants, yielding values ranging from 0.0098 to 0.0103 N/m.

1. Menozzi, F.D. *et al.* Identification of a heparin-binding hemagglutinin present in mycobacteria. *J. Exp. Med.* **184**, 993–1001 (1996).
2. Pethe, K. *et al.* Characterization of the heparin-binding site of the mycobacterial heparin-binding hemagglutinin adhesin. *J. Biol. Chem.* **275**, 14273–14280 (2000).
3. Reddy, V.M. & Kumar, B. Interaction of *Mycobacterium avium* complex with human respiratory epithelial cells. *J. Infect. Dis.* **181**, 1189–1193 (2000).
4. Menozzi, F.D., Bischoff, R., Fort, E., Brennan, M.J. & Locht, C. Molecular characterization of the mycobacterial heparin-binding hemagglutinin, a mycobacterial adhesin. *Proc. Natl. Acad. Sci. USA* **95**, 12625–12630 (1998).
5. Pethe, K. *et al.* The heparin-binding haemagglutinin of *M. tuberculosis* is required for extrapulmonary dissemination. *Nature* **412**, 190–194 (2001).
6. Mueller-Ortiz, S.L. *et al.* Decreased infectivity despite unaltered C3 binding by a ΔhbhA mutant of *Mycobacterium tuberculosis*. *Infect. Immun.* **70**, 6751–6760 (2002).
7. Delogù, G. & Brennan, M.J. Functional domains in the mycobacterial hemagglutinin, HBHA. *J. Bacteriol.* **181**, 7464–7469 (1999).
8. Binnig, G., Quate, C.F. & Gerber, C. Atomic force microscope. *Phys. Rev. Lett.* **56**, 930–933 (1986).
9. Engel, A. & Müller, D.J. Observing single biomolecules at work with the atomic force microscope. *Nat. Struct. Biol.* **7**, 715–718 (2000).
10. Hörber, J.K. & Miles, M.J. Scanning probe evolution in biology. *Science* **302**, 1002–1005 (2003).
11. Dufrêne, Y.F. Using nanotechniques to explore microbial surfaces. *Nat. Rev. Microbiol.* **2**, 451–460 (2004).
12. Lee, G.U., Chrisey, L.A. & Colton, R.J. Direct measurement of the forces between complementary strands of DNA. *Science* **266**, 771–773 (1994).
13. Hinterdorfer, P., Baumgartner, W., Gruber, H.J., Schilcher, K. & Schindler, H. Detection and localization of individual antibody-antigen recognition

events by atomic force microscopy. *Proc. Natl. Acad. Sci. USA* **93**, 3477–3481 (1996).

14. Lower, S.K., Hochella, M.F. & Beveridge, T.J. Bacterial recognition of mineral surfaces: nanoscale interactions between *Shewanella* and α-FeOOH. *Science* **292**, 1360–1363 (2001).

15. Abu-Lail, N.I. & Camesano, T.A. Elasticity of *Pseudomonas putida* KT2442 surface polymers probed with single-molecule force microscopy. *Langmuir* **18**, 4071–4081 (2002).

16. Ludwig, M., Dettmann, W. & Gaub, H.E. Atomic force microscope imaging contrast based on molecular recognition. *Biophys. J.* **72**, 445–448 (1997).

17. Heinz, W.F. & Hoh, J.H. Spatially resolved force spectroscopy of biological surfaces using the atomic force microscope. *Trends Biotechnol.* **17**, 143–150 (1999).

18. Grandbois, M., Dettmann, W., Benoit, M. & Gaub, H.E. Affinity imaging of red blood cells using an atomic force microscope. *J. Histochem. Cytochem.* **48**, 719–724 (2000).

19. Lehenkari, P.P., Charras, G.T., Nykänen, A. & Horton, M.A. Adapting atomic force microscopy for cell biology. *Ultramicroscopy* **82**, 289–295 (2000).

20. Almqvist, N. *et al.* Elasticity and adhesion force mapping reveals real-time clustering of growth factor receptors and associated changes in local cellular rheological properties. *Biophys. J.* **86**, 1753–1762 (2004).

21. Luk, Y-Y. *et al.* Using liquid crystals to amplify protein-receptor interactions: design of surfaces with nanometer-scale topography that present histidine-tagged protein receptors. *Langmuir* **19**, 1671–1680 (2003).

22. Rief, M., Oesterhelt, F., Heymann, B. & Gaub, H.E. Single molecule force spectroscopy on polysaccharides by atomic force microscopy. *Science* **275**, 1295–1297 (1997).

23. Merkel, R., Nassoy, P., Leung, A., Ritchie, K. & Evans, E. Energy landscapes of receptor-ligand bonds explored with dynamic force spectroscopy. *Nature* **397**, 50–53 (1999).

24. Baumgartner, W. *et al.* Cadherin interaction probed by atomic force microscopy. *Proc. Natl. Acad. Sci. USA* **97**, 4005–4010 (2000).

25. Auletta, T. β-Cyclodextrin host-guest complexes probed under thermodynamic equilibrium: thermodynamics and AFM force spectroscopy. *J. Am. Chem. Soc.* **126**, 1577–1584 (2004).

26. Devadoss, P., Klegerman, M.E. & Groves, M.J. Surface morphology of *Mycobacterium bovis* BCG: relation to mechanisms of cellular aggregation. *Microbios.* **65**, 111–125 (1991).

27. Florin, E.L., Moy, V.T. & Gaub, H.E. Adhesion forces between individual ligand-receptor pairs. *Science* **264**, 415–417 (1994).

28. Margalit, H., Fischer, N. & Ben-Sasson, S.A. Comparative analysis of structurally defined heparin binding sequences reveals a distinct spatial distribution of basic residues. *J. Biol. Chem.* **268**, 19228–19231 (1993).

29. Bernfield, M. *et al.* Functions of cell surface heparan sulfate proteoglycans. *Annu. Rev. Biochem.* **68**, 729–777 (1999).

30. Tkachenko, E. & Simons, M. Clustering induces redistribution of syndecan-4 core protein into raft membrane domains. *J. Biol. Chem.* **277**, 19946–19951 (2002).

31. Ofek, I., Hasty, D.L. & Sharon, N. Anti-adhesion therapy of bacterial diseases: prospects and problems. *FEMS Immunol. Med. Microbiol.* **38**, 181–191 (2003).

Corrigendum: Nanoscale mapping and functional analysis of individual adhesins on living bacteria

Vincent Dupres, Franco D Menozzi, Camille Locht, Brian H Clare, Nicholas L Abbott, Stéphane Cuenot, Coralie Bompard, Dominique Raze & Yves F Dufrêne
Nat. Methods **2**, 515–520 (2005).

The web address for the Leproma world-wide web server has been changed (http://genolist.pasteur.fr/Leproma/).